Tribology Letters (2018) 66:92
https://doi.org/10.1007/s11249-018-1039-5

ORIGINAL PAPER

Shear Thinning and Hydrodynamic Friction of Viscosity Modifier-Containing Oils. Part I: Shear Thinning Behaviour

Nigel Marx[1] · Luis Fernández[2] · Francisco Barceló[2] · Hugh Spikes[1]

Received: 24 February 2018 / Accepted: 11 June 2018 / Published online: 21 June 2018

Abstract
Viscosity versus shear rate curves have been measured up to 10^7 s^{-1} for a range of VM solutions and fully formulated oils of known composition at several temperatures. This shows large differences in the shear thinning tendencies of different engine oil VMs. It has been found that viscosity versus shear rate data at different temperatures can be collapsed onto a single master curve using time–temperature superposition based on a shear rate shift factor. This enables shear thinning equations to be derived that are able to predict the viscosity of a given oil at any shear rate and temperature within the range originally tested. One of the tested lubricants does not show this time temperature superposition collapse. This fluid also exhibits extremely high viscosity index and shear thins more easily at high than at low temperature, unlike all the other solutions tested. This unusual response may originate from the presence on the VM molecules of two structurally and chemically different components. In a companion paper, the master shear thinning curves obtained in this paper are used to explore how VMs impact film thickness and friction in a steadily loaded, isothermal journal bearing [1].

Keywords Viscosity modifier · Viscosity index improver · Shear thinning

1 Introduction

Viscosity modifier additives are used to increase the viscosity index of lubricants and are key components of most crankcase engine oils. It is well known that their blends exhibit shear thinning at the high shear rates present in lubricated contacts and that the resulting reduction in viscosity leads to thinner lubricant films and lower hydrodynamic friction than predicted in the absence of shear thinning.

This paper describes measurement of the temporary shear thinning behaviour of a range of engine oil viscosity modifier (VM) additive solutions. By using three different viscometers, full flow curves of viscosity versus shear rate are obtained at several temperatures and fitted to various shear thinning equations. It is found that for almost all of the VMs, time–temperature superposition enables the shear thinning behaviour at all temperatures to be described by a single equation.

In a companion paper, the master shear thinning curves obtained in this paper are used to explore how VMs impact film thickness and friction in a steadily loaded, isothermal journal bearing [1].

2 Background

Viscosity index improver polymers or viscosity modifiers (VMs) have been used as engine oil additives since the mid-1930s [2]. In recent years, their application has extended to gear oils, automatic transmission fluids, greases and some hydraulic fluids. Their primary role is to enhance the lubricant viscosity index of their blends by making a greater proportionate contribution to blend viscosity at high than at low temperature [3, 4]. This enables the development of multigrade engine oils that combine a reasonably low viscosity at low engine temperature with sufficient viscosity at high temperature to produce effective hydrodynamic films in engine components. High viscosity index also contributes to engine efficiency by providing low viscosity and thus low hydrodynamic friction at low temperatures. A recent paper has reviewed VMs and how they impart function [5].

✉ Hugh Spikes
h.spikes@imperial.ac.uk

[1] Imperial College London, London, UK

[2] Repsol Technology Centre, Madrid, Spain

Engine oil VMs are polymers with molecular weights typically in the range 300–700 k. As such they can exhibit both permanent and temporary shear thinning at the high shear rates present in engine components including the ring pack and journal bearings. Permanent shear thinning or permanent viscosity loss results from the thermomechanical scission of the VM polymer chains at the high shear stresses present in lubricated contacts and is, as the name suggests, irreversible, resulting in a permanent reduction in viscosity of the lubricant [6]. Temporary shear thinning is generally believed to result from conformational changes, such as partial alignment of the VM polymer molecules in solution under shear, that reduce the interactions between solvent/polymer and polymer/polymer molecules and thus the blend viscosity [7]. The low shear rate viscosity is recovered fully after cessation of shear.

Permanent shear thinning is almost always undesirable since it can eventually result in the oil falling out of its intended viscosity grade. It generally sets the upper limit of VM molecular weight that can be used in a lubricant for a specific application. Initially, temporary shear thinning was also unwelcome since it leads to a reduction in hydrodynamic film thickness. However, it is now recognised that in hydrodynamic lubricated contacts, temporary shear thinning of engine oils is beneficial for fuel economy and that this may more than offset the negative impact of reduced film thickness.

As will be shown in this study, the temporary shear thinning behaviour of VM-containing engine oils occurs typically over the shear rate range 10^4 to 10^8 s^{-1} and for many years it was not possible to reach shear rates above *ca* 10^6 s^{-1} in high shear viscometers. This meant that the shear thinning behaviour of VM solutions could not be fully explored. Typical flow curves of engine oils up to 10^6 s^{-1} can be found in [8–11]. This limitation has recently been addressed by the development of the PCS ultrashear viscometer (USV) that is able to reach 10^7 s^{-1}. This enables almost entire shear thinning curves to be obtained for VMs representative of those used in engine oils at realistic concentrations and temperatures. Full flow curves of two engine oils obtained in this way are described by Taylor [12]. To date, this approach has not been used to explore and compare the shear thinning properties of different VMs. Such information is, however, important for designing low friction engine oils. This paper therefore describes a systematic study of the temporary shear thinning properties of a range of commercial VM blends, both in simple solutions and in fully formulated engine oils. The measured shear thinning behaviour is then used in conjunction with a conventional isothermal hydrodynamic lubrication model in the companion paper to explore how and the extent to which shear thinning influences film thickness and friction in a journal bearing [1].

3 Test Oils

Seventeen VM blends were studied, denoted in this paper as #1 to #17, and described in Tables 1 and 2. All met viscosity classification 15W40. Fluids #1 to #10 were simple solutions of different commercial viscosity modifier polymers (VMs) in the same 6 cSt API Group II base oil. Their compositions are listed in Table 1. The VM concentrations listed are those of the VM concentrate and not the raw polymer. All blends had raw polymer concentration in the range 1–2% wt. except for oils #7 and #10 which contained 5 and 6% raw polymer, respectively. For all VMs, blends were prepared at various polymer concentrations around the value finally used and these all showed blend viscosity to increase linearly with polymer concentration, indicative of the dilute polymer solution regime. All blends were formulated to have an HTHS (dynamic

Table 1 Ten blends of base oil with VM

Oil	VM type	VM wt.%	VM structure	Base oil type	BOV (cSt)@100C	HTHS (cP)
#1	SIP	11.5	Star	G-II	6	3.73
#2	SIP	26.0	Star	G-II	6	3.71
#3	SIP	10.0	Star	G-II	6	3.71
#4	SIP	25.0	Linear diblock	G-II	6	3.70
#5	A-OCP	11.5	Linear	G-II	6	3.69
#6	A-OCP	13.5	Linear	G-II	6	3.71
#7	D-PMA	9.0	Linear	G-II	6	3.70
#8	A-OCP	11.5	Linear	G-II	6	3.76
#9	SBR	24.0	Linear diblock	G-II	6	3.75
#10	PMA	13.5	Comb	G-II	6	3.77

SIP hydrogenated styrene isoprene, *OCP* olefin copolymer, *PMA* polymethacrylate, *SBR* hydrogenated styrene butadiene, *D*- dispersant-, *A*- amorphous

Table 2 Seven blends of base oil + VM + DI

Oil #	DI pack	DI pack wt%	VM	VM wt%	Base oil type	BOV@100C (cSt)	HTHS (cP)
#11	D1	11.9	VM in #2	15.7	G-II	6	3.73
#12	D1	11.9	VM in #2	17.2	G-III	6	3.69
#13	D1	11.9	VM in #2	19.7	G-IV	6	3.68
#14	D1	11.9	VM in #2	4.6	G-II	8.5	3.73
#15	D1	11.9	VM in #9	4.2	G-II	8.5	3.70
#16	D1	11.9	VM in #6	2.2	G-II	8.5	3.73
#17	D2	12.35	VM in #9	5.7	G-II	8.5	3.72

viscosity at shear rate 10^6 s^{-1}, 150 °C) of 3.7 ± 0.06 cP. The VMs in oils #5 and #8 were nominally the same additive from different suppliers.

Fluids #11 to #17 were blends of base oil, VM and a commercial detergent-inhibitor (DI) package, as listed in Table 2. All had an HTHS of 3.7 ± 0.06 cP. Blends #11 to #13 had the same VM in three different base oils, a Group II, Group III and Group IV, respectively. Blends #14 to #17 were all based on an 8.5 cSt Group II base oil, #14 to #16 containing the same DI pack but three different VMs and #15 and #17 having different DI packs but the same VM.

Several VM-free oils were also tested, as listed in Table 3. Fluid #18 was an additive-free Group IV base oil blended to have an HTHS of 3.7 cSt and thus serves as a polymer-free, Newtonian reference oil for comparison with the VM-containing oils. Also studied were the four base oils employed in blending; the 6 cSt base oil used in blends #1 to #11, denoted #1–11b; the Group III and Group IV base oils used to blend #12 and #13, respectively, denoted #12b and #13b; and the 8.5 cSt Group II base oil of #14 to #17, denoted #14–17b. Finally, DI-containing but VM-free versions of #11 to #17 were also studied and are denoted #11b + DI, #14–16b + DI and #17b + DI.

4 Methods

Flow curves spanning the range *ca* 10 s^{-1} up to 10^7 s^{-1} were determined for all test fluids at 60, 80, 100 and 120 °C. Each flow curve comprises three types of measurement.

4.1 Low Shear Rate Viscosity Measurement (*ca* 10 to 100 s^{-1})

Viscosities at low shear rate were measured using a Stabinger viscometer (SVM3000). This is a horizontal, concentric cylinder device in which an outer cylinder is rotated and a free-floating inner cylinder is braked and the torque measured using an eddy current method. The shear rate is not precisely defined and depends on the fluid viscosity, but is in the range 1 to 10^3 s^{-1}. All of the oils studied are assumed to be at their first Newtonian viscosity up to 10^3 s^{-1}. The viscometer was also used to measure fluid density based on the oscillating U-tube method. Measurements of dynamic viscosity and density were made at five temperatures over the range 20–100 °C.

In the current study, the SVM3000 was used in a conventional fashion except that a well-defined calibration fluid, squalane, was employed since this has been found to provide reliable and transferable results. The precision of the

Table 3 Base oil and DI blends

Oil #	DI pack	DI pack wt%	Base oil type	BOV @100C (cSt)	HTHS (cP)
#18 (ref)	–	–	G-IV	12.3	3.70
#1–11b	–	–	G-II	6	2.08
#12b	–	–	G-III	6	–
#13b	–	–	G-IV	6	–
#14–17b	–	–	G-II	8.5	–
#11b + DI	D1	11.9	G-II	6	–
#12b + DI	D1	11.9	G-III	6	–
#13b + DI	D1	11.9	G-IV	6	–
#14–16b + DI	D1	11.9	G-II	8.5	–
#17b + DI	D2	12.35	G-II	8.5	–

measurements obtained for the VM oils is believed to be ±0.5%.

4.2 High Shear Rate Viscosity Measurement (5×10^5 to 10^7 s^{-1})

These measurements were made with a PCS Instruments USV. This is a vertically oriented, concentric cylinder device with a rotating inner cylinder and typically a 1 to 2 µm gap, as shown schematically in Fig. 1.

The key problem in measuring viscosities at shear rates greater than *ca*. 10^6 s^{-1} is shear heating. Very large amounts of heat are generated due to shear and these cause a rapid and uncontrollable temperature rise of the bounding surfaces. In the USV, this is overcome by rotating the inner cylinder for less than 0.1 s, over which time this temperature rise is very small. A motor accelerates a flywheel to high speed and then a clutch system engages to transmit the rotational energy to the inner cylinder (rotor) for just a few revolutions at a set shear rate. Depending on the lubricant viscosity and thus the shear stress applied, a small amount of shear heating may still occur within this time frame, but based on the shear stress the USV calculates this. It then reduces the temperature of the chamber slightly so that the lubricant sample reaches the sought test temperature in subsequent measurements. Three further engagement-disengagement cycles are then carried out and the resulting three torque measurements are averaged.

Another problem with measuring engine oil viscosity at very high shear rates is permanent viscosity loss due to polymer breakdown. In practice most engine oil VMs show such breakdown at shear rates above 10^6 s^{-1}, so that successive viscosity measurements made on the same sample at high shear rate show a progressive reduction in viscosity as permanent shear thinning accumulates. This phenomenon can be utilised to study the permanent shear thinning of polymer solutions [13]. To address this problem in the current study, a new polymer sample was used for each combination of shear rate and temperature by flushing the previously used sample 10 times with fresh polymer solution. Also, for each condition, a series of three viscosity measurements were made in succession (each consisting of 4 cycles). As illustrated in Fig. 2, at very high shear rates these showed a slight but significant progressive viscosity decrease and the three viscosity values were back-extrapolated to provide the initial, non-permanent shear-thinned viscosity value.

The results provided in this study are believed to be ±2% in the normal 10^6 to 10^7 s^{-1} shear rate range of the USV. However, measurements were also extended below this range down to 5×10^5 s^{-1} and these are ±5%.

4.3 Mid Shear Rate Viscosity Measurement (ca 3×10^4 to 3×10^5 s^{-1})

Since considerable VM solution temporary shear thinning can occur below 5×10^5 s^{-1}, it was important to measure viscosities in the mid shear rate range. For this, a USV with an abnormally large gap (14 µm) was used. The frictional torque produced at these lower shear rates is considerably less than at shear rates above 10^6 s^{-1} and this provided a lower limit of shear rate at which viscosity could be measured.

At shear rates below 10^6 s^{-1}, permanent shear thinning is not an issue, so successive measurements were made at different shear rates and temperatures on a single test sample. Between test oils, the USV was partially disassembled and the rotor and stator cleaned using solvents in an ultrasonic bath and then dried. Measurements have precision ±5%.

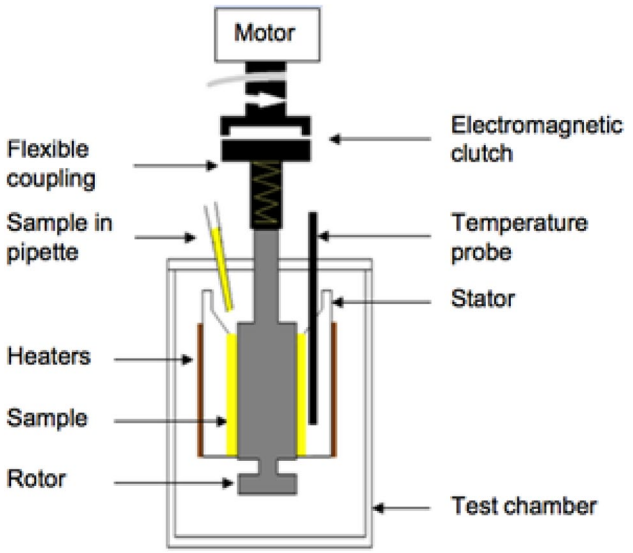

Fig. 1 Schematic diagram of USV viscometer

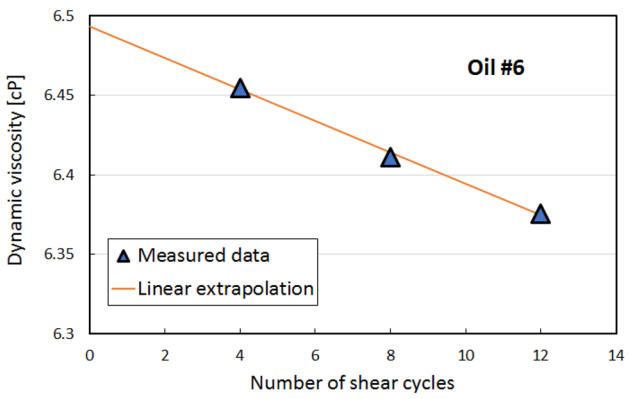

Fig. 2 Permanent shear thinning behaviour to illustrate back-extrapolation, oil #6, shear rate 6×10^6 s^{-1}, 100 °C

5 Low Shear Rate Viscosity

5.1 Viscosities

Dynamic viscosities and densities were measured at 20, 40, 60, 80 and 100 °C using the Stabinger viscometer. Viscosity at 120 °C was calculated from these using ASTM 341 and assuming a linear variation of density with temperature. Tables 4, 5 and 6 list the kinematic viscosities at 40 and 100 °C and the VIs of the test oils. Viscosity indices (VI) were calculated from the kinematic viscosities at 40 and 100 °C using ASTM D2270-10(2016). Also listed are constants a_o, b_o and c_o of the Vogel viscosity-temperature equation;

$$\eta_o = a_o e^{b_o/(T-c_o)} \quad (1)$$

These were obtained from best fits to the five measured low shear rate dynamic viscosities.

For all the VM blends, the addition of the viscosity modifier has the effect of increasing VI. However from Table 4, it can be seen that the different VMs give strikingly different viscosity indices, ranging from 149 to 276 for the simple VM solutions, #1 to #10, and 125 to 180 for the fully formulated oils, #11 to #17.

Table 4 Low shear rate viscometrics of test oils #1 to #10 (simple VM blends)

Test oil	KV40C (cSt)	KV100C (cSt)	VI	Vogel a_o (cP)	Vogel b_o (°C)	Vogel c_o (°C)
#1	107.26	16.19	162.3	0.11158	989.308	− 107.84
#2	75.28	14.94	209.9	0.31383	673.581	− 87.17
#3	96.22	15.01	163.9	0.09507	1022.25	− 111.6
#4	124.69	19.91	182.6	0.12945	1028.18	− 113.64
#5	90.29	13.60	152.8	0.0844	1024.21	− 110.63
#6	100.96	15.22	158.8	0.10288	995.216	− 108.31
#7	66.42	12.54	191	0.161106	850.124	− 105.28
#8	89.98	13.36	149.3	0.08168	1025.42	− 110.11
#9	94.88	15.73	177.2	0.10438	1021.68	− 113.94
#10	42.35	11.40	276.2	1.13028	310.73	− 50.628

Table 5 Low shear rate viscometrics of test oils #11 to #17 (VM + DI blends)

Test oil	KV40C (cSt)	KV100C (cSt)	VI	Vogel a_o (cP)	Vogel b_o (°C)	Vogel c_o (°C)
#11	79.50	13.73	177.9	0.19964	770.535	− 92.505
#12	72.81	12.93	180.2	0.14727	858.854	− 102.66
#13	72.93	12.70	175.4	0.09726	999.662	− 115.6
#14	92.66	12.58	131.4	0.0646	1054.26	− 108.11
#15	95.77	12.64	127.3	0.07005	1025.97	− 105.35
#16	100.52	12.99	125.7	0.06667	1045.59	− 106.07
#17	95.19	12.73	129.8	0.07264	1021.2	− 105.47

Table 6 Low shear rate viscometrics of VM-free oils

Test oil	KV40C (cSt)	KV100C (cSt)	VI	Vogel a_o (cP)	Vogel b_o (°C)	Vogel c_o (°C)
#1–11b (base)	35.89	6.05	114.2	0.06322	883.001	− 103.24
#18 (ref)	82.98	12.48	147.7	0.04839	1193.38	− 124.72
#12b	32.89	6.02	130.7	0.05961	923.484	− 111.03
#13b	31.59	6.02	139.7	0.04642	1025.33	− 122.46
#14–17b	60.86	8.58	113.3	0.05863	971.583	− 103.46
#11b + DI	53.51	8.26	126.1	0.06495	955.742	− 105.9
#12b + DI	47.89	8.06	140.5	0.06241	985.286	− 112.49
#13b + DI	45.62	7.97	147.0	0.04807	1088.63	− 123.47
#14–16b + DI	85.96	11.27	119.4	0.061271	1030.284	− 105.4
#17b + DI	82.61	10.90	118.5	0.05969	1031.48	− 105.77

5.2 Thickening Power

The ability of the polymer to thicken the solvent to which it is added can be defined as

$$TP = \frac{\eta_o - \eta_s}{\eta_s} \quad (2)$$

where η_o is the low shear rate dynamic viscosity of the VM solution and η_s that of the solvent. *TP* is also often called the "specific viscosity".

Figure 3 compares thickening power (*TP*) as a function of temperature for the VM solutions #1 to #10. The symbols for oil #5 are largely obscured by those of oil #8, which is as expected since the two VMs are believed to be the same.

Some of the VMs show *TP* that decreases with temperature while blends #2, #7 and #10 show *TP* that increases with temperature. The behaviour of oil #10 is particularly striking with the polymer contributing only very slightly to viscosity at low temperatures but proportionately much more at high temperatures. Consequently oil #10 features a very high VI.

It is sometimes assumed that since VMs increase viscosity index, they must show a thickening power that increases with temperature. Figure 3 indicates that this is not the case and that VI can increase even when thickening power decreases with temperature. In a recent review, Martini et al. described the various ways that a VM can increase thickening power as temperature increases but also noted that the definition of viscosity index means that the addition of a VM can increase viscosity index even if none of these occur [5].

Figure 4 shows the thickening power of the polymers in base oil + DI blends #11 to #17. In these, the solvent viscosity η_s corresponds to the viscosity of the respective base oil + DI mixture. It should be noted that the y-axis scale is only one-third that of Fig. 3, indicating that the VM blends with DI package have much lower *TP*s. This is because the VM concentrations are considerably lower since the DI package contributes to the blend viscosity. There is also a clear difference between the three blends based on 6 cSt base oils and those formulated with an 8.5 cSt oil because the latter have lower VM concentrations and thus lower *TP*s than the former.

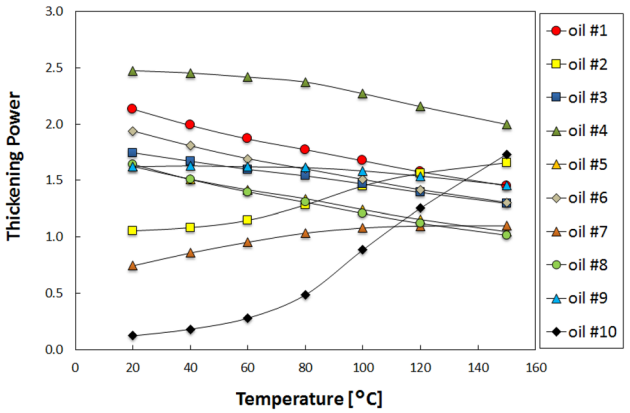

Fig. 3 Viscosity thickening power of the VMs in oils #1 to #10

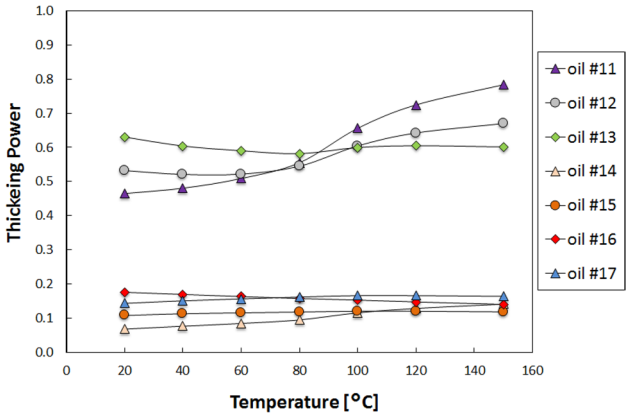

Fig. 4 Viscosity thickening power of the VMs in oils #11 to #17

Figure 5 compares formulations with the same VM and DI pack in three different base oils, Group II (oil #11), Group III (oil #12) and Group IV (oil #14). Also shown is oil #2, which has the same VM in Group II base oil but no DI pack (and thus a higher VM concentration). The impact of the higher concentration of polymer in the DI-free formulation is evident. The *TP* increases with temperature for the Group II and Group III oils but not the Group IV.

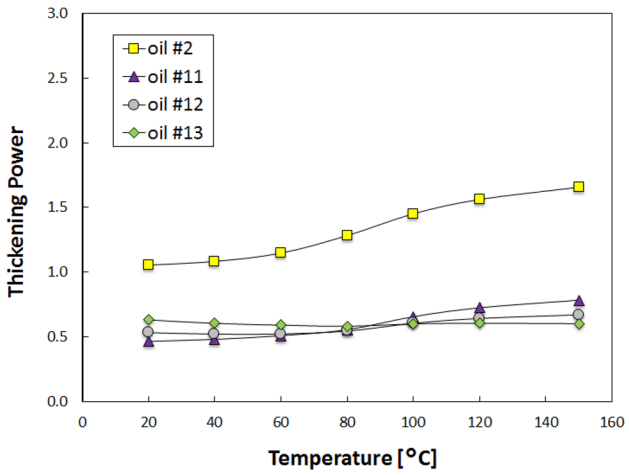

Fig. 5 Viscosity thickening power against temperature when adding a DI package or changing the base oil group

6 High Shear Rate Viscosity Results

6.1 Flow Curves of VM Blends #1 to #10

Figure 6 shows a set of viscosity versus shear rate curves for oil #1 at four temperatures. These illustrate classical polymer solution shear thinning behaviour with a Newtonian response at low shear rate (the first Newtonian), a progressive reduction in viscosity at intermediate shear rates, trending to a second Newtonian at very high shear rate. It should be noted that the first two data points at 100 and 500 s^{-1} in this and subsequent figures both originate from the Stabinger viscometer and are shown as two separate points simply to establish visually the presence of the first Newtonian.

The solid lines shown in Fig. 6 are best fits to each data set of the Carreau-Yasuda shear thinning equation [14].

$$\eta = \eta_\infty + \left(\eta_o - \eta_\infty\right)\left(1 + (A\dot{\gamma})^a\right)^{\left(\frac{n-1}{a}\right)} \tag{3}$$

where η is the dynamic viscosity of the fluid at shear rate $\dot{\gamma}$; η_o is the first Newtonian viscosity; η_∞ is the second Newtonian viscosity and A, n and a are constants of fit. A has units of seconds and can be regarded as a relaxation time. n is always less that unity and typically 0.2–0.9, while a is generally between 1.0 and 2.0. The Carreau-Yasuda equation reduces to the Carreau equation if $a = 2$. The value of η_∞ should lie very slightly above the viscosity of the polymer-free formulation η_s. Since this was not known for the current oils, for #1 to #10 the base oil viscosity has been used for η_∞.

The Carreau-Yasuda equation is one of the several equations used to describe the temporary shear thinning of polymer solutions; alternative equations will be discussed in Sect. 7.3 of this paper.

All the test oils gave similarly shaped flow curves. Figures 7 and 8 compare viscosity *versus* shear rate data at 60 and 120 °C, respectively, for all ten VM-containing oils #1 to #10. All test oils show temporary shear thinning at shear rates above *ca* 10^4 s^{-1}.

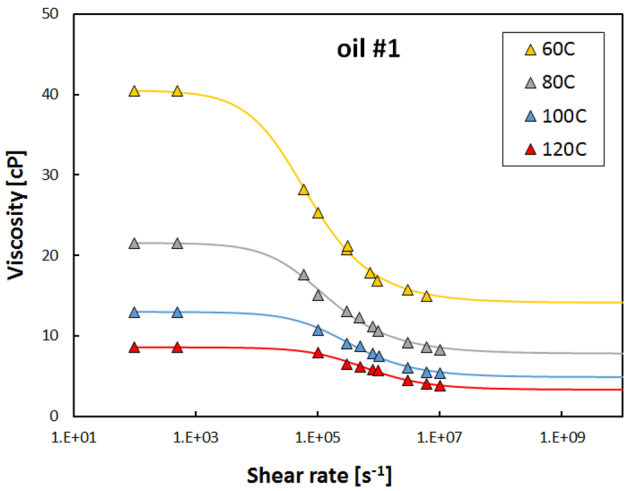

Fig. 6 Flow curves of oil #1 at four temperatures

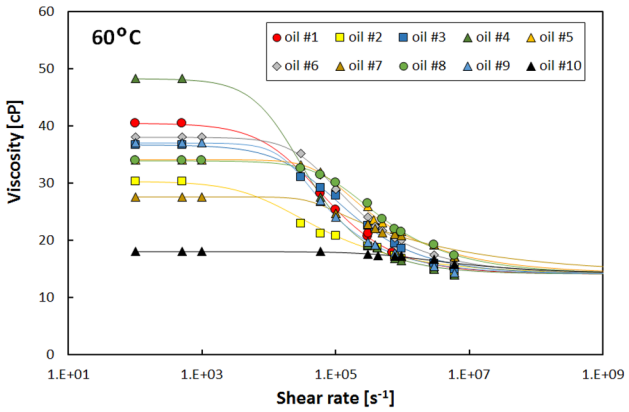

Fig. 7 Flow curves of ten VM solutions at 60 °C

Because of their much higher viscosities at low temperature, the viscosity loss of these VM solutions at low temperatures appears much higher than at high temperature. A useful comparative value that compensates for this is the fractional viscosity loss, expressed as the ratio of the polymer thickening at high shear rate, $\left(\eta - \eta_\infty\right)$, to that at low shear rate, $\left(\eta_o - \eta_\infty\right)$. This is termed the shear stability index, *SSI*, and normalises the viscosity axis to lie between unity (first Newtonian) and zero (second Newtonian).

$$SSI = \frac{\eta - \eta_\infty}{\left(\eta_o - \eta_\infty\right)}. \tag{4}$$

The Carreau-Yasuda equation can be rearranged to relate *SSI* directly to shear rate;

$$SSI = \frac{\left(\eta - \eta_\infty\right)}{\left(\eta_o - \eta_\infty\right)} = \left(1 + (A\dot{\gamma})^a\right)^{\left(\frac{n-1}{a}\right)}. \tag{5}$$

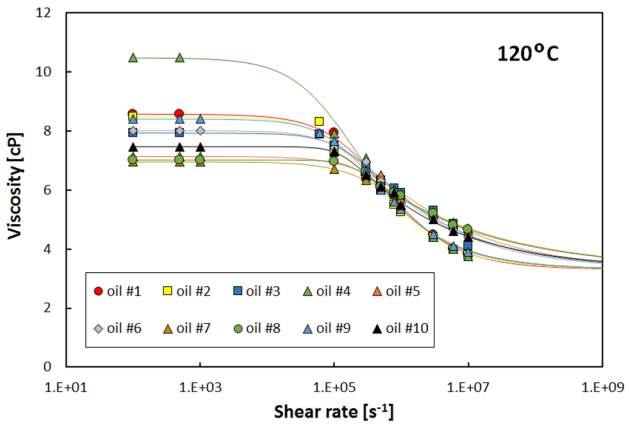

Fig. 8 Flow curves of ten VM solutions at 120 °C

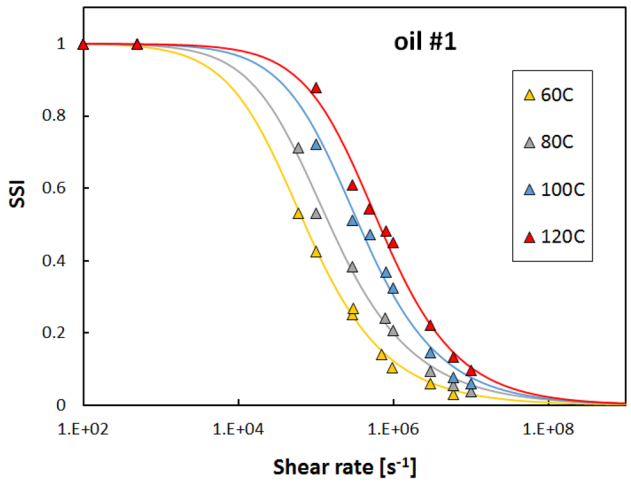

Fig. 9 SSI versus shear rate for oil #1 at four temperatures

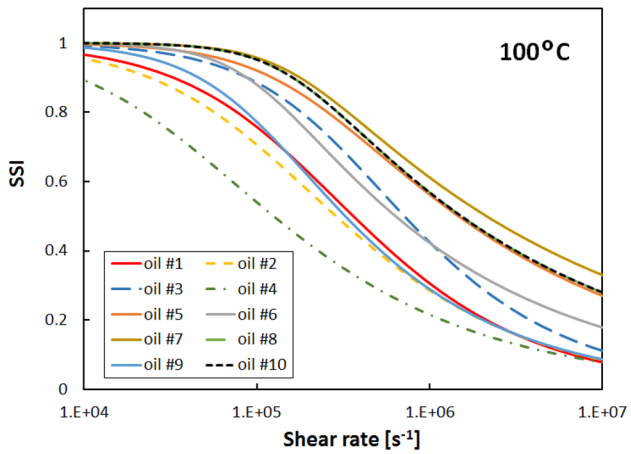

Fig. 10 SSI *versus* shear rate for #1 to #10 at 100 °C

Figure 9 shows SSI versus shear rate plots for oil #1 at four temperatures. It illustrates clearly how the occurrence of shear thinning moves to higher shear rate as the temperature is increased. Almost all VM-containing oils tested showed a similar behaviour.

Figure 10 compares Carreau-Yasuda SSI versus shear rate fits for all ten VM solutions at 100 °C, focussing on the shear rate range 10^4 to 10^7 s^{-1}. There is a considerable spread, with oil #4 shear thinning much more readily than oil #7. In this figure, oils #1 and #9 almost coincide, as do oils #5, #8 and #10. Clearly oils #4, #2, #1 and #9 shear thin at lower shear rates than the other blends.

6.2 Flow Curves of VM + DI Blends #11 to #17

Figure 11 shows flow curves for the VM + DI blend, oil #11.

These are of similar form to the VM-only blends but show a smaller drop in viscosity at high shear rates. This is simply

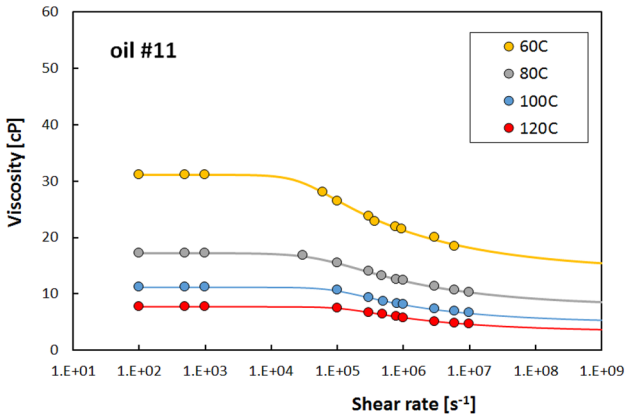

Fig. 11 Flow curves of oil #11 at four temperatures

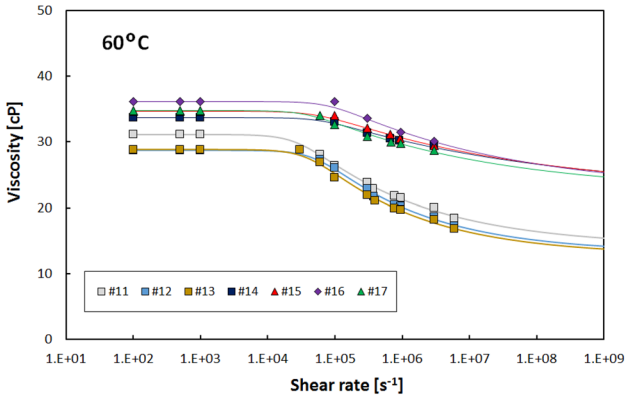

Fig. 12 Flow curves of seven VM + DI solutions at 60 °C

because there is less VM present (oil #11 has 15.7% wt. as compared to 26% wt. of the same VM in oil #2) due to the thickening contribution of the DI pack. Figure 12 compares the flow curves of all seven VM + DI blends at 60 °C. Oils #11 to #13 are formulated with a 6 cSt base oil while # 14 to #17 have an 8.5 cSt base oil. The latter have low VM concentration and thus show relatively little shear thinning.

As with the simple VM blends, the measured viscosities of the VM + DI blends can be converted to SSIs to normalise the effect of variations in bulk viscosity due to base oil and temperature. There is, however, an issue with choice of the second Newtonian viscosity, η_∞ in Eq. 4. Ideally the latter should correspond to the low shear rate viscosity of the solvent, i.e. that of the base oil + DI pack blend and SSIs calculated using this are shown in Fig. 13. This indicates almost complete polymer shear thinning at very high shear rates, similar to the VM blends. However, as shown in Fig. 14, small but significant amounts of shear thinning of the DIs themselves occur at shear rates above 10^6 s^{-1}. This may originate from the dispersant and/or overbased detergent in the DI packs. It has the effect of slightly reducing the calculated

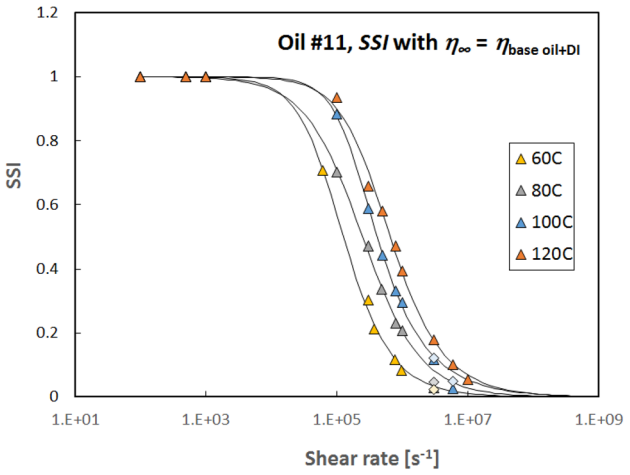

Fig. 13 SSI versus shear rate of oil #11. SSIs calculated based on η_∞ being the base oil + DI viscosity (diamond symbols are based on η_∞ being the high shear rate viscosity of the base oil + DI)

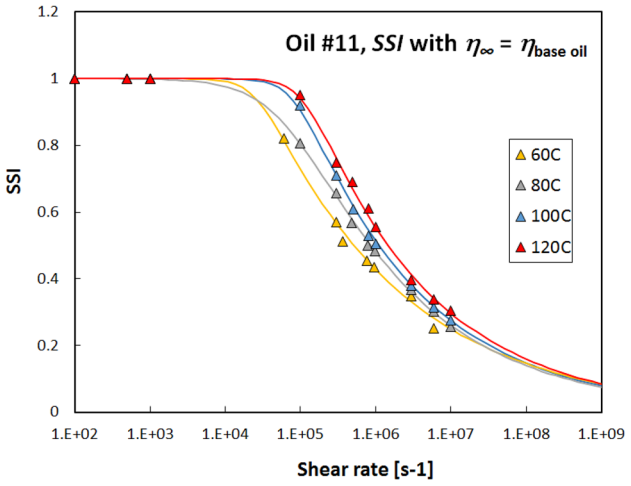

Fig. 15 SSI versus shear rate of oil #11. SSIs calculated based on η_∞ being the base oil viscosity

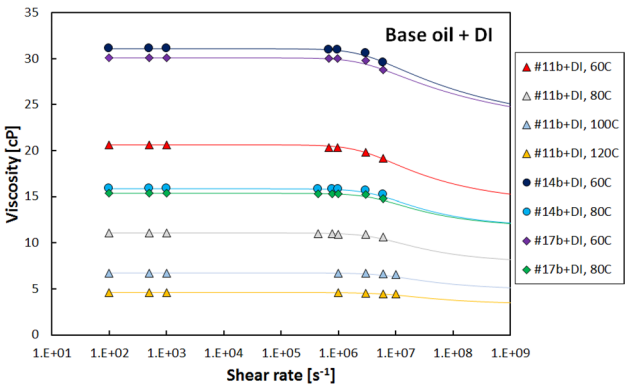

Fig. 14 Flow curves for base oil + DI blends showing shear thinning of the DI packs

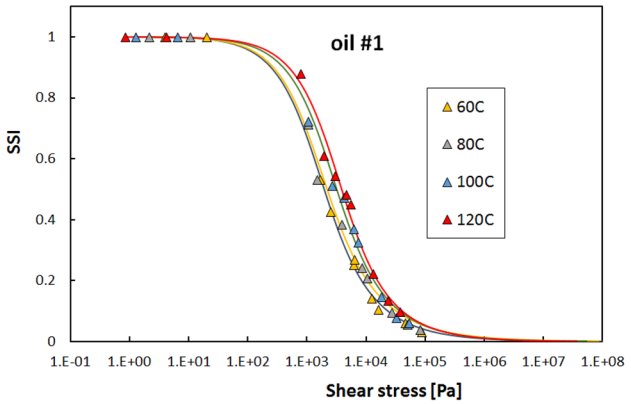

Fig. 16 SSI versus shear stress for oil #1 at four temperatures

SSI at high shear rates in Fig. 13. The diamond symbols in Fig. 13 show SSIs calculated based on η_∞being the viscosity of the DI solution (11b + DI) at the prevailing shear rate; it can be seen that this correction is quite small.

An alternative approach is to calculate SSI taking the second Newtonian viscosity, η_∞ to be the base oil viscosity and this is shown in Fig. 15. In this case, the SSI falls only to about 20% at the highest shear rate, with the residual thickening being mainly due to the DI pack.

7 Discussion of Shear Thinning Results

7.1 Temperature Scaling of Flow Curves

Were it possible to scale the flow curves measured at different temperatures to lie on a single collapsed curve for a given blend, then a resulting equation of fit could be used to generate flow curves at any temperature. Since shear thinning has been suggested to originate from the shear stress experienced by the fluid and not the shear rate [15], a version of the Carreau-Yasuda equation has been proposed in which the shear rate is replaced by the shear stress, τ, experienced by the solution [16].

$$SSI = \frac{\eta - \eta_\infty}{(\eta_o - \eta_\infty)} = \left(1 + \left(\frac{\tau}{G}\right)^a\right)^{\left(\frac{n-1}{a}\right)}, \quad (6)$$

where G is critical shear stress around which shear thinning occurs. The *SSI* is plotted against shear stress (measured viscosity × shear rate) for oil #1 in Fig. 16. It has the effect of bringing closer together the different temperature curves but there remains a slight, almost linear shift with

increasing temperature, possibly due to the constant G in Eq. 6 varying with temperature.

In polymer theory, viscoelastic responses at different temperatures, including shear thinning behaviour, are often combined into one data set using "time–temperature shifting" or "time–temperature superposition" (TTS). In this, all relaxation modes of the polymer are considered to scale in the same way with temperature, so that any relaxation mode, λ_i, at temperature T is given by

$$\lambda_{i(T)} = a_T \lambda_{i(T_R)}, \tag{7}$$

where a_T is a time scale shift factor and T_R is a reference temperature where $a_T = 1$. If polymers collapse in this way, they are said to be *thermo-rheologically simple* [17].

For polymer melts at atmospheric pressure a_T is generally taken to be [17]

$$a_T = \frac{\eta_{o(T)}}{\eta_{o(T_R)}} . \frac{T_R}{T}. \tag{8}$$

For polymer solutions, the situation is less clear. Some authors have suggested Eq. 9 [17, 18];

$$a_T = \frac{\left[\eta_o - \eta_s\right]_{(T)}}{\left[\eta_o - \eta_s\right]_{(T_R)}} . \frac{T_R}{T} \tag{9}$$

and this is adopted in the current study. However, shear rate shifting based on the solvent viscosity has also been proposed [19];

$$a_T = \frac{\eta_{s(T)}}{\eta_{s(T_R)}} . \frac{T_R}{T}. \tag{10}$$

According to TTS, polymer viscoelastic data should collapse along the x-axis if the frequency (in our case shear rate) data are converted to a reduced form by multiplying by a_T. The y-axis stress data (in our case viscosity) may also be scaled by multiplying by $1/a_T.T/T_R$, but this is not necessary when using SSI since the viscosity value has already been normalised.

Figure 17 shows the effect of applying TTS to oil #1, taking the reduced shear rate to be $\dot{\gamma}_r = a_T \dot{\gamma}$, where a_T is given by Eq. 9 and the reference temperature is 60 °C. This transformation aligns the results at all temperatures closely. All but one of the VM solutions tested gave equally good or better collapse onto a single curve. Figure 18 shows *SSI* versus reduced shear rate for oil #6 and Fig. 19 shows oils #5 and #8. The latter were believed to be the same VM, though sourced from different suppliers, and indeed they both fall on a single curve. Oils #1 and #3 (and also oils #2, #4 and #9) shear-thinned almost completely under the most severe

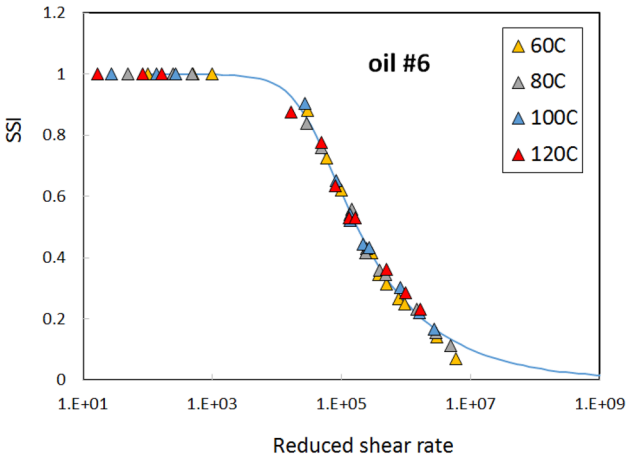

Fig. 18 SSI versus reduced shear rate for oil #6

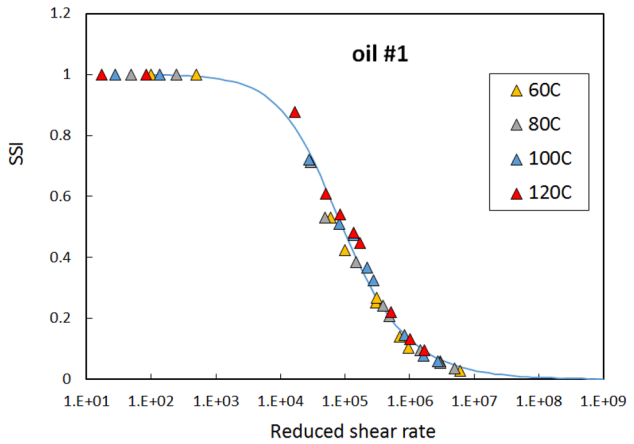

Fig. 17 SSI versus reduced shear rate for oil #1

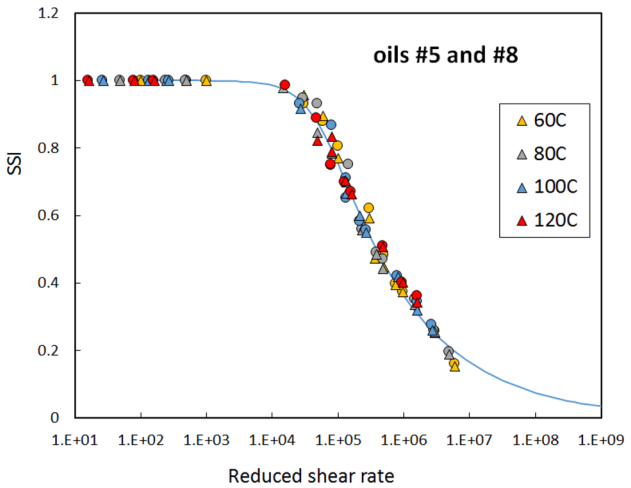

Fig. 19 SSI versus reduced shear rate for oil #5 and oil #8

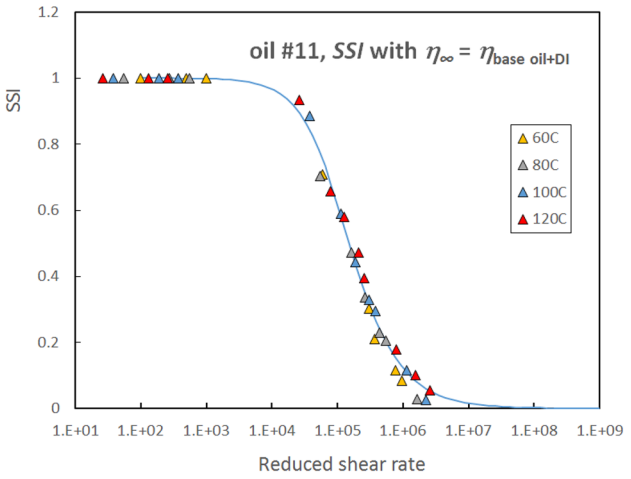

Fig. 20 SSI versus reduced shear rate for oil #11. SSIs calculated based on η_∞ being the base oil + DI viscosity

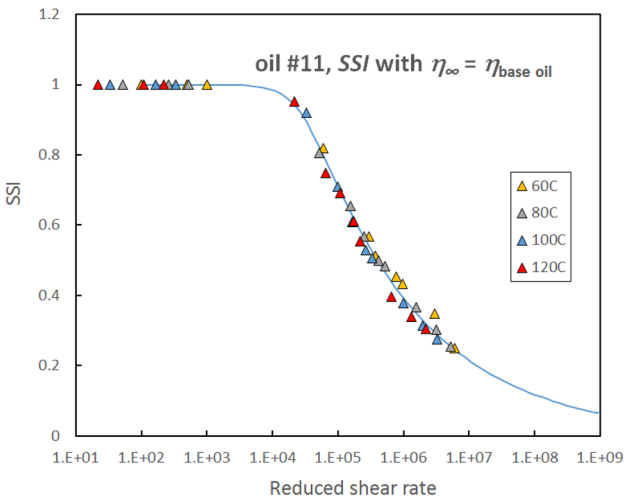

Fig. 21 SSI versus reduced shear rate for oil #11. SSIs calculated based on η_∞ being the base oil

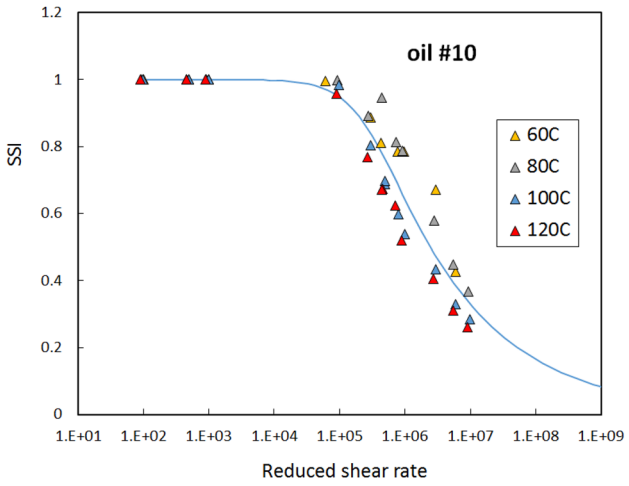

Fig. 22 SSI versus reduced shear rate for oil #10

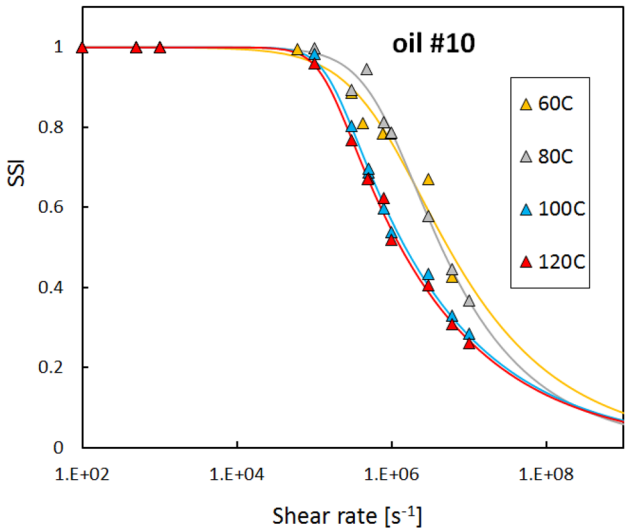

Fig. 23 SSI *versus* shear rate for oil #10 showing that the blend shear thins more readily at high than at low temperature

conditions studied. However, as seen in Fig. 19, oils #5 and #8 shear-thinned less readily so the SSI did not approach zero at the highest shear rate. This was also the case for oils #6, #7 and #10.

Full collapse onto a single curve was also seen for all the seven VM + DI blends. Figures 20 and 21 show this for oil #11, with the SSI defined in terms of η_∞ being the low shear rate viscosity of the base oil + DI pack and just the base oil viscosity, respectively.

The only VM solution that did not collapse onto a single curve when *SSI* was plotted against reduced shear rate was oil #10, as shown in Fig. 22. This suggests that this VM is not thermo-rheologically simple. Haley and Lodge have discussed reasons why dilute polymer solutions might not be thermo-rheologically simple [20]. Essentially, this may occur when the polymer contains molecular components whose dynamics have different temperature dependencies. The VM in oil #10 has a comb structure where the backbone of the comb is believed to have a different chemistry from the side chains and this may contribute to the observed thermal response. Figure 23 shows that, unlike all of the other polymers solutions studied, oil #10 shear thins more easily at high than at low temperatures, implying that the polymer molecules become more susceptible to shear alignment as temperature rises from 80 to 100 °C. Indeed, when the reduced Carreau-Yasuda equation is fitted to the four individual sets of viscosity *versus* reduced shear rate measurements made at different temperatures, the values of A are similar for 60 and 80 °C, and then show a sharp increase to

a value about four times larger at 100 and 120 °C, implying a sudden increase in relaxation time. This polymer solution also has extremely high VI and examination of Table 4 shows that its Vogel constants are very different from the other fluids.

7.2 Carreau-Yasuda Fit Constants

The solid lines shown in Figs. 17, 18, 19, 20, 21 and 22 are best fits of the reduced Carreau-Yasuda equation

$$SSI = \left(1 + (A_r\dot{\gamma}_r)^{a_r}\right)^{\left(\frac{n_r-1}{a_r}\right)}, \tag{11}$$

where the reduced shear rate is $\dot{\gamma}_r = a_T\dot{\gamma}$ and $a_T = \frac{[\eta_o-\eta_\infty]_{(T)}}{[\eta_o-\eta_\infty]_{(T_R)}}.\frac{T_R}{T}$. T is the absolute test temperature and T_R is the absolute reference temperature, 313 K (60 °C). $[\eta_0 - \eta_\infty]_{(T)}$ and $[\eta_0 - \eta_\infty]_{(T_R))}$ are the differences between the first and second Newtonian values at the test temperature and the reference temperature, respectively. The Carreau-Yasuda constants have suffixes r to indicate that they are based on reduced shear rates.

Although the Carreau-Yasuda fit is good over most of the shear rate range, for most oils the measured SSI falls more sharply at very high shear rate (when SSI < 0.1) than predicted by the Carreau-Yasuda equation. This may arise from a limitation in the Carreau-Yasuda equation or from the VM carrier fluid having lower viscosity than the base oil, so reducing the second Newtonian slightly below the latter's viscosity. It should be noted that the Carreau-Yasuda equation has not, to the authors' knowledge, previously been tested over this wide a range of SSIs.

Tables 7 and 8 list the reduced Carreau-Yasuda constants of best fit for all of the VM-containing oils tested. For all except oil #10, these constants can be used in Eq. 12 to predict the viscosity of each oil at any shear rate and temperature within the measurement range.

$$\eta = \eta_\infty + \left(\eta_o - \eta_\infty\right)\left(1 + (A_r\dot{\gamma}_r)^{a_r}\right)^{\left(\frac{n_r-1}{a_r}\right)} \tag{12}$$

The η_o values at the test temperature and the reference temperature in Eq. 12 can be determined using the Vogel constants from Table 4 or 5 while the η_∞ values can be determined in the same way from the solvent Vogel constants in Table 6. For the DI-containing oils, two sets of fit constants are listed in Table 8, one based on best fits taking the second Newtonian viscosity η_∞ used to determine a_T to be the viscosity of the base oil employed and the other taking it to be the viscosity of the base oil + DI pack.

Oil #10 is included in Table 7 but it is not recommended that this fit be used; the quite high R^2 value listed for this oil is misleading since it fails to indicate that the data at different temperatures have not collapsed fully. Instead the fits at individual temperatures are listed in Table 9.

To test the validity of this approach for predicting high shear rate viscosity, the fit constants in Tables 7 and 8 were

Table 7 Reduced Carreau-Yasuda constants for ten oils #1 to #10

Test oil	A_r (μs)	n_r	a_r	R^2
#1	21.88	0.36	1.00	0.990
#2	78.52	0.64	2.50	0.970
#3	10.96	0.40	1.00	0.986
#4	68.39	0.47	1.00	0.991
#5	18.41	0.66	1.52	0.993
#6	30.90	0.60	1.58	0.996
#7	21.13	0.75	2.26	0.991
#8	19.72	0.67	1.80	0.989
#9	34.28	0.47	1.37	0.996
#10	3.76	0.69	1.34	0.901

Reference temperature $T_R = 60$ °C

Table 8 Reduced Carreau-Yasuda constants for seven VM + DI oils #11 to #17

Test oil	Solvent (to calculate η_∞)	A_r (μs)	n_r	a_r	R^2
#11	1–11b	39.36	0.75	2.50	0.995
#12	12b	31.99	0.75	2.13	0.986
#13	13b	33.11	0.75	2.50	0.992
#14	14–17b	24.27	0.88	2.50	0.972
#15	14–17b	26.92	0.88	2.50	0.963
#16	14–17b	26.92	0.88	2.13	0.975
#17	14–17b	25.12	0.84	2.50	0.976
#11	11b + DI	8.91	0.05	1.24	0.994
#12	12b + DI	8.91	0.14	1.34	0.984
#13	12b + DI	14.45	0.31	1.67	0.991
#14	14–16b + DI	9.89	0.05	2.50	0.941
#15	14–16b + DI	13.96	0.14	2.50	0.951
#16	14–16b + DI	12.59	0.31	1.73	0.968
#17	17b + DI	11.35	0.05	2.50	0.959

Reference temperature $T_R = 60$ °C

Table 9 Carreau-Yasuda constants for oil #10 at four test temperatures

Test temperature (°C)	η_o (cP)	η_∞ (cP)	A (μs)	n	a
60	18.04	14.129	1.29	0.67	1.00
80	11.61	7.793	1.08	0.58	1.31
100	9.19	4.872	6.10	0.69	2.00
120	7.47	3.311	6.53	0.68	2.00

used in conjunction with the Vogel constants in Tables 4 and 5 to predict the viscosity of each oil at 10^6 s^{-1} and 150 °C (the HTHS conditions). For all oils, the predicted viscosity was within 10% of the measured HTHS values listed in Tables 1 and 2, even though the latter were not used in the fit procedure. The average deviation for all the test oils was 4.5% and equally good predictions were obtained using the base oil and the base oil + DI pack fit constants in Table 8. It should be noted that this is quite a stringent test since; (a) for all test oils the fits were based on temperatures up to only 120 °C, so prediction at 150 °C involved extrapolation; (b) as can be seen in Fig. 7, the viscosities vary rapidly with shear rates around 10^6 s^{-1}.

7.3 Alternative Shear Thinning Equations

Thus far, curve fitting to the flow curves has employed the Carreau-Yasuda shear thinning equation, Eq. 3. This was used since its three disposable parameters guarantee a good fit and the main goal of the work was to show how shear thinning equations can be obtained for prediction of engine component hydrodynamic behaviour. It is however an empirically based equation and interaction between its fit constants can obscure the significance of each individual constant in terms of its contribution to shear thinning behaviour. There are many alternative shear thinning equations in the literature [21–23] and for polymer solutions these can all be rearranged into expressions describing SSI in terms of shear rate. Three alternative equations are listed below. In these, the constants A denote relaxation times and these and the other constants have been given different suffixes to emphasise that they may not represent the same value in the various equations.

Carreau [24];

$$SSI = \left(1 + (A_1\dot{\gamma}_r)^2\right)^{\left(\frac{n_1-1}{2}\right)} \tag{13}$$

Cross [25, 26];

$$SSI = \left(1 + (A_2\dot{\gamma}_r)^{n_2}\right)^{-1} \tag{14}$$

Powell-Eyring [27, 28];

$$SSI = \frac{\sinh^{-1}(A_3\dot{\gamma}_r)}{A_3\dot{\gamma}_r} \tag{15}$$

Whereas Carreau-Yasuda is based on three disposable constants, Carreau and Cross are based on two and the Powell-Eyring equation on only one. In principle, all can be expressed in terms of reduced shear rate and best fits for each of these equations to the reduced flow curves of oil #1 are shown in Fig. 24. It is evident that all fit the data quite closely so it is thus not possible to use the data measured in this study to support any specific shear thinning equation. From Fig. 24, it can be seen that the region where shear thinning begins is important in determining closeness of fit and more data would be desirable in this region. Shear thinning in this relatively low shear rate region will depend on the presence of high molecular weight molecules and thus on the polydispersity of the polymer. Ree, Ree and Eyring [29] and Yasuda [30] have discussed how to extend the Eying and Carreau equations, respectively, to allow for mixtures of components with different relaxation times.

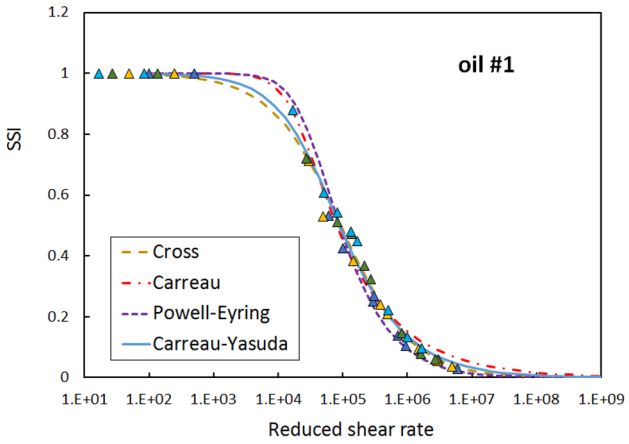

Fig. 24 Comparison of best fits of four shear thinning equations to SSI versus reduced shear rate data for oil #1

The ability to derive a single equation (Eq. 12) to describe the shear thinning of a given VM blend is important since it enables quantification of the impact of VM on shear thinning over a wide range of conditions and can also be used in modelling of the hydrodynamic behaviour of VM blends in hydrodynamic lubricated components, as described in the companion paper, Part 2 [1].

8 Conclusions

To study the temporary shear thinning of multigrade oils, viscosity versus shear rate curves have been measured up to 10^7 s^{-1} for a range of simple VM solutions and fully formulated engine oils of known composition at several temperatures. For measurements at shear rates above 10^6 s^{-1}, it is essential to take account of and eliminate effects due to permanent shear thinning and this can be done by shearing a test sample several times in succession and charting the permanent loss of viscosity.

The study has shown that there are large differences in the temporary shear thinning tendencies of different engine oil VMs.

Shear stability index, SSI, is a useful way to normalise the shear thinning results of fluid of different viscosity for

comparison purposes. This reveals clearly the effect of temperature on shear thinning and aids in comparison of different VMs.

For almost all VM solutions, viscosity versus shear rate data at different temperatures can be collapsed onto a single master curve using time temperature superposition based on a shear rate shift factor. This enables shear thinning equations to be derived that describe the viscosity of a given oil at any shear rate and temperature within the range originally tested. Such equations can be used to explore the impact of shear thinning on engine and other lubricated components and thus enable the informed design and selection of lubricants to optimise rheological performance [1].

Acknowledgements The authors would like to thank Repsol S.A. for supporting this work and supplying base fluids and additives and PCS Instruments for help in setting up the mid-shear range USV.

References

1. Marx, N., Fernández, L., Barceló, F., Spikes, H.A.: Shear thinning and hydrodynamic friction of viscosity modifier-containing oils. Part II: impact of shear thinning on journal bearing friction. Tribol. Lett. (2018). https://doi.org/10.1007/s11249-018-1040-z
2. Boehm, A.B.: Lubricating-oil improvers. Proc. API Annual Meeting **28**(2), 35–41 (1948)
3. Mueller, H.G.: Mechanism of action of viscosity index improvers. Trib Intern. **11**, 189–192 (1978)
4. Covitch, M.J., Trickett, K.J.: How polymers behave as viscosity index improvers in lubricating oils. Adv. Chem. Eng. Sci. **5**(02), 134–151 (2015)
5. Martini, A., Ramasamy, U.S., Len, M.: Review of viscosity modifier lubricant additives. Tribol. Lett. **66**, 58 (2018)
6. Wood, L.G.: The change of viscosity of oils containing high polymers when subjected to high rates of shear. Br. J. Appl. Phys. **1**, 202–206 (1950)
7. Selby, T.W.: The non-Newtonian characteristics of lubricating oils. ASLE Trans. **1**, 68–81 (1958)
8. Bates, T.W., Williamson, B., Spearot, J.A., Murphy, C.K.: A correlation between engine oil rheology and oil film thickness in engine journal bearings, SAE Technical Paper 860376 (1986)
9. Rhodes, R.B.: Development of ASTM standard test methods for measuring engine oil viscosity using rotational viscometers at high-temperature and high-shear rates. High-Temperature, High-Shear Oil Viscosity: Measurement and Relationship to Engine Operation. ASTM International, pp. 14–22 (1989)
10. Tolton, T.J.: The viscosity losses of new and sheared multi weight oil formulations determined at multiple shear rates. SAE Tech. Paper 890727 (1989)
11. Sorab, J., Holdeman, H.A., Chui, G.K.: Viscosity prediction for multigrade oils. SAE Technical Paper 932833 (1993)
12. Taylor, R.I., de Kraker, B.R.: Shear rates in engines and implications for lubricant design. Proc. Inst. Mech. Eng. Part J. **231**, 1106–1111 (2017)
13. Marx, N., Ponjavic, A., Taylor, R.I., Spikes, H.A.: Study of permanent shear thinning of VM polymer solutions. Tribol. Lett. **65**, 106 (2017)
14. Yasuda, K.Y., Armstrong, R.C., Cohen, R.E.: Shear flow properties of concentrated solutions of linear and star branched polystyrenes. Rheol. Acta **20**, 163–178 (1981)
15. Horowitz, H.H.: Predicting effects of temperature and shear rate on viscosity of viscosity index-improved lubricants. Ind. Eng. Chem. **50**, 1089–1094 (1958)
16. Bair, S.: A rough shear-thinning correction for EHD film thickness. Tribol. Trans. **47**, 361–365 (2004)
17. Bird, R.B.: Dynamics of Polymeric Liquids: Fluid Mechanics vol. 1. Chapter 3.6. 2nd edn. Wiley, Hoboken (1987)
18. Tanner, R.I.: Engineering Rheology Second Edition. Oxford University Press, Oxford (2000)
19. Phan-Thien, N.: On the time-temperature superposition principle of dilute polymer liquids. J. Rheol. **23**, 451–456 (1979)
20. Haley, J.C., Lodge, T.P.: Failure of time-temperature superposition in dilute miscible polymer blends. Coll. and Polymer Sci. **282**, 793–801 (2004)
21. Wright, B., Van Os, N.M., Lyons, J.A.: European activity concerning engine oil viscosity classification-part IV-the effects of shear rate and temperature on the viscosity of nultigrade oils. SAE Technical Paper 830027 (1983)
22. Cho, Y.I., Kensey, K.R.: Effects of the non-Newtonian viscosity of blood on flows in a diseased arterial vessel. Part 1: steady flows. Biorheology **28**, 241–262 (1991)
23. Bair, S., Qureshi, F.: The generalized Newtonian fluid model and elastohydrodynamic film thickness. Trans. ASME J. Tribol. **125**, 70–75 (2003)
24. Carreau, P.J.: Rheological equations from molecular network theories. Trans. Soc. Rheol. **16**, 99–127 (1972)
25. Cross, M.M.: Rheology of non-Newtonian fluids: a new flow equation for pseudo plastic systems. J. Coll. Sci. **20**, 417–437 (1965)
26. Dobson, G.R.: Analysis of high shear rate viscosity data for engine oils. Tribol. Intern. **14**, 195–198 (1981)
27. Powell, R.E., Eyring, H.: Mechanism for relaxation theory of viscosity. Nature **154**, 427–428 (1944)
28. Talbot, A.F.: High shear viscometry of concentrated solutions of poly (alkylmethacrylate) in a petroleum lubricating oil. Rheol. Acta **13**, 305–317 (1974)
29. Ree, F., Ree, T., Eyring, H.: Relaxation theory of transport problems in condensed systems. Ind. Eng. Chem. **50**, 1036–1040 (1958)
30. Yasuda, K.: A multi-mode viscosity model and its applicability to non-Newtonian fluids. J. Text. Eng. **52**, 171–173 (2006)